Acta Mech
DOI 10.1007/s00707-012-0711-3

Vali Parvaneh · Mahmoud Shariati · Hamid Torabi

Bending buckling behavior of perfect and defective single-walled carbon nanotubes via a structural mechanics model

Received: 21 July 2010 / Revised: 1 April 2012

Abstract A structural mechanics model is employed for the investigation of the bending buckling behavior of perfect and defective single-walled carbon nanotubes (SWCNTs). The effects of different types of defects (vacancies and Stone–Wales defects) at various locations on the critical bending buckling moments and curvatures are also studied for zigzag and armchair nanotubes with various aspect ratios (length/diameter). The locations of defects are along the length of the nanotube and around the circumference. Moreover, the results of this structural mechanics model are compared with a finite element model. The simple continuum model, especially, could be adopted to predict the critical buckling moments and curvatures of SWCNTs with large aspect ratio. Finally, the results of the present structural model are compared with those from molecular dynamics (MD) simulation, and there is good agreement between our model and the MD model.

1 Introduction

In 1991, Ijima [1] discovered carbon nanotubes (CNTs) by chance while studying manufacturing methods for fullerenes. Carbon nanotubes excited interest in nanoscale materials research mainly because of their unusual mechanics structure. This led to extensive research on carbon nanotubes as components of nanomechanics devices. Wang et al. [2] used an advanced finite element analysis package, ABAQUS, and found the relationship of the nonlinear bending moment–curvature of carbon nanotubes. They also utilized this relationship and a nonlinear vibration analysis method that captured the rippling deformation on the inner arc of the bent nanotube to show that the effective bending modulus of carbon nanotubes decreases substantially with increasing diameter. An extensive finite element analysis was carried out by Yao et al. [3] to investigate the buckling behaviors of SWCNTs and MWCNTs under bending deformation. They showed the relationships between the bending buckling loads and the bending angle or curvature for CNTs with the geometrical parameters, such as tube diameter, length, and chirality. Guo et al. [4] employed the atomistic-scale finite element method to study the bending buckling of single-walled carbon nanotubes. The simulation showed that the appearance of kinks associated with the large deformation nearby reduces the slope of the strain energy curve in the post-buckling stages and hence increases the flexibility of the SWCNTs. Leung et al. [5] proposed the idea of "spatial periodic strain" and obtained a rational equivalent relationship and achieved an efficient model, which links the

V. Parvaneh (✉)
Department of Engineering, Islamic Azad University, Shahrood Branch, Shahrood, Iran
E-mail: vali.parvaneh@gmail.com

M. Shariati
Department of Mechanical Engineering, Shahrood University of Technology, Daneshgah Blvd, Shahrood, Iran

H. Torabi
Young Researchers Club, Mashhad Branch, Islamic Azad University, Mashhad, Iran

Published online: 02 August 2012

molecular mechanics with the continuum mechanics. Their model is another improvement of the model of Odegard et al. [6].

Han et al. [7] studied the instability of a double-walled carbon nanotube embedded in an elastic medium with pure bending. The effects of the surrounding elastic medium and the Van der Waals forces between the inner and outer nanotubes were taken into account. Based on their model, they derived a model in terms of the buckling modes of the shell from which the critical bending moment can be predicted. Sun and Liew [8] studied the bending buckling of single-walled carbon nanotubes in the theoretical scheme of the higher-order gradient continuum. They also developed a mesh-free method to implement the numerical modeling of SWCNTs and simulated their bending buckling behavior numerically with the developed method.

Due to the application of carbon nanotubes in various industries such as NEMS, a mechanical analysis of these nanotubes under different loading and boundary conditions is necessary. Among these analyses, bending buckling is very important. Thus, we have tried to predict the critical bending buckling moments of SWCNTs. The method employed for this analysis is a structural mechanics approach. Different defects may exist in carbon nanotubes, which have an effect on the critical bending buckling moments. Therefore, the influence of various vacancy and Stone–Wales defects is also investigated in the analysis.

2 Simulation method

2.1 Application of the structural model to SWCNTs

We have proposed a structural mechanics method to model the carbon nanotubes. The detailed derivation procedure for the formulation and other features of this model can be found in our previous work [9].

The total steric potential energy due to interactions between carbon atoms can be represented by Eq. (1) [10]:

$$u_{\text{total}} = u_r + u_\theta + u_\phi + u_\omega \tag{1}$$

where u_r, u_θ, u_ϕ, and u_ω are bond energies associated with bond stretching, angle variation or bond bending, dihedral angle torsion, and out-of-plane torsion, respectively.

In this model, Morse potentials are employed for stretching and bending potentials, and a periodic type of bond torsion is applied for torsion and out-of-plane torsion interactions (Eqs. 2– 5),

$$u_r = D_e \left\{ \left[1 - e^{-\beta(r-r_0)} \right]^2 - 1 \right\}, \tag{2}$$

$$u_\theta = \frac{1}{2} k_\theta (\theta - \theta_0)^2 \left[1 + k_{\text{sextic}} (\theta - \theta_0)^4 \right], \tag{3}$$

$$u_\phi = \frac{1}{2} k_\phi \left[1 + \cos\left(n\phi - \phi_0 \right) \right], \tag{4}$$

$$u_\omega = \frac{1}{2} k_\omega \left[1 + \cos\left(n\omega - \omega_0 \right) \right]. \tag{5}$$

As indicated in Figs. 1a and 2, a nonlinear axial spring is used for modeling of the angle variation interaction between atoms. The relationship between changes in the bond and the corresponding change in length of the spring for small displacements can be expressed simply by Eq. (6) [6],

$$\Delta\theta \approx \frac{2\,(\Delta R)}{r_0}, \quad r_0 = 0.142 \text{ nm} \tag{6}$$

Therefore, we can simplify Eq. (3)–(6):

$$u_\theta = \frac{2}{r_0^2} k_\theta \, (R - R_0)^2 \left[1 + \frac{16}{r_0^4} k_{\text{sextic}} (R - R_0)^4 \right]. \tag{7}$$

The stretch force, the angle variation moment, the dihedral angle torque, and out-of-plane torque can be obtained from differentiations of Eqs. (2), (7), (4), (5) as functions of bond stretch, bond angle, dihedral angle, and out-of-plane angle variation, respectively:

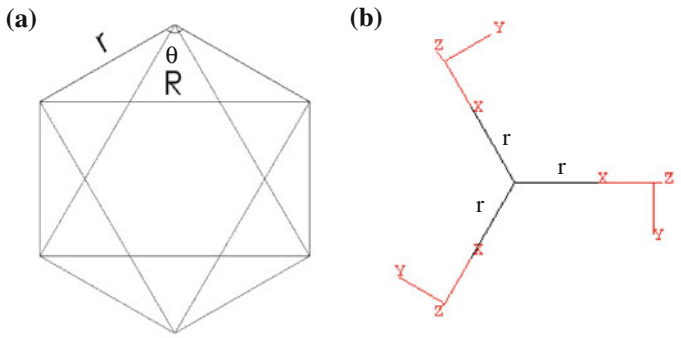

Fig. 1 **a** A hexagonal unit cell, **b** location of local coordinates of each connector

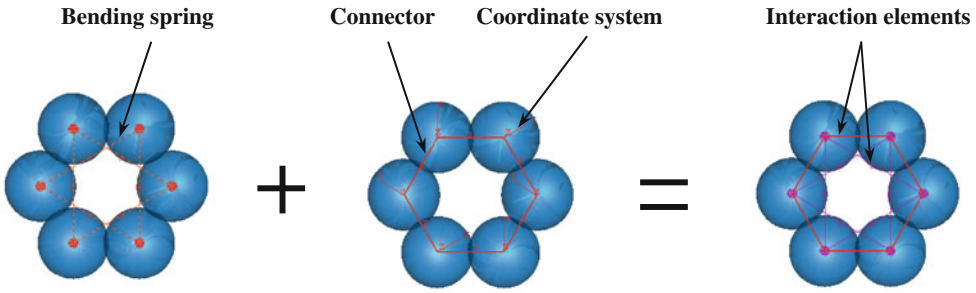

Fig. 2 Spring and connector elements corresponding to the interactions of carbon atoms. **a** The angle variation interactions, **b** the stretching and torsional interactions, **c** total interactions

$$F(r - r_0) = 2\beta D_e \left[1 - e^{-\beta(r-r_0)}\right] e^{-\beta(r-r_0)}, \tag{8}$$

$$F(R - R_0) = \frac{4}{r_0^2} k_\theta (R - R_0) \left[1 + \frac{16}{r_0^4}\left(1 + \frac{4}{r_0^2}\right) k_{\text{sextic}} (R - R_0)^4\right], \tag{9}$$

$$T(\phi - \phi_0) = \frac{1}{2} k_\phi n \sin(n\phi - \phi_0), \tag{10}$$

$$T(\omega - \omega_0) = \frac{1}{2} k_\omega n \sin(n\omega - \omega_0). \tag{11}$$

A nonlinear connector is considered for modeling of the stretching and torsional interactions and a nonlinear spring for modeling of the angle variation interaction (see Fig. 2). Carbon atoms in ABAQUS are modeled by a discrete rigid sphere so that connector elements between atoms are adjoined to reference points at the center of the sphere, and a local coordinate is set at the center of each atom (see Figs. 1b, 2). This local coordinate is a combination of a Cartesian coordinate for stretching and a rotational coordinate for torsion. The X direction of these coordinates is in the connector direction, and the Z direction is vertical to the central axis of the nanotube. Because we can only use a linear spring in the CAE space of ABAQUS, by changing the linear spring command to a nonlinear spring command in the input file, and by applying the nonlinear data for $F(\Delta R)$ versus ΔR using Eq. (9), we can apply the bond bending spring to the model. For applying bond stretch and torsion forces to the connectors, we can apply the nonlinear stiffnesses in three directions (X, Y, Z) directly. For stretching stiffness in the X direction, we can obtain the nonlinear data for $F(\Delta r)$ versus Δr by Eq. (8), and for torsional stiffness in X direction, we can obtain the nonlinear data for $T(\Delta\phi)$ versus $\Delta\phi$ by Eq. (10). For torsional stiffness in the Y direction, we can obtain the nonlinear data for $T(\Delta\omega)$ versus $\Delta\omega$ by Eq. (11).

Here, we take $E = 1,170$ GPa and $\nu = 0.196$ for the Young's modulus and Poisson's ratio of single-walled carbon nanotubes, respectively. We used $k_r = 800$ nN/nm, $k_\theta = 1.42$ nN/nm Rad^{-2}, $k_\phi = k_\omega = 0.0418$ nN nm, which are consistent with the values reported in the literature [11,12]. This structural model was successfully used for predicting the mechanical properties and axial buckling behavior of single-walled carbon nanotubes. It is employed here for the bending buckling of single-walled carbon nanotubes.

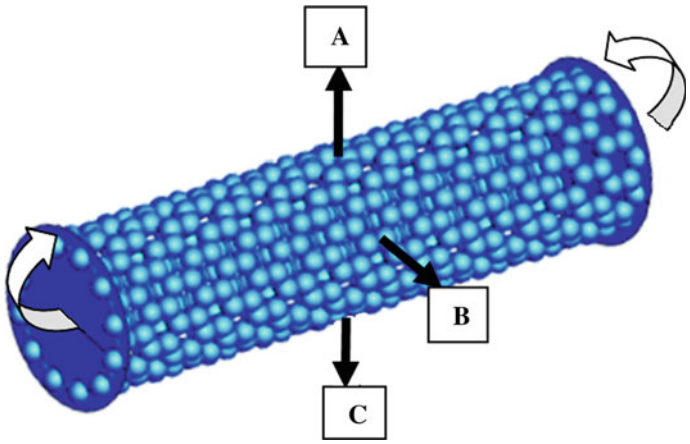

Fig. 3 Configuration of simulated single-walled carbon nanotube with the loading, boundary conditions, and location of defects (A, B, and C) in ABAQUS

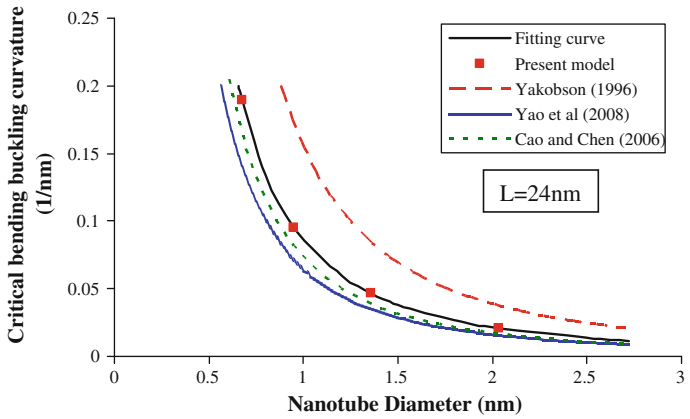

Fig. 4 Variation of the critical bending buckling curvature with diameter for SWCNT. The tube length is fixed at 24 nm

3 Results and discussion

The critical bending buckling moments and curvatures as well as the influence of vacancy and Stone–Wales defects were predicted by our structural model. Zigzag (12,0) and armchair (7,7) nanotubes with various aspect ratios (L/d) were employed for this study. First, we fixed the tow planes at the ends of the nanotube and applied a moment to the center of the tow planes (see Fig. 3).

It is seen from Fig. 4 that the feature of the diameter-dependent critical bending buckling curvature is captured by the present model, and the critical bending buckling curvature decreases with increasing tube diameter. The solid line is the fitting line using the formula $\kappa_{\mathrm{cr}} = a/d^2$ line. The present fitted value of a is 0.08574 nm.

To verify the above described model, in Fig. 4, we have compared the present results to those of Yakobson et al. [13], Cao and Chen [14] and Yao et al. [3]. From this figure, it can be found that the present results of zigzag model are very close to those of Cao and Chen [14]. Their calculated fitted value of a is 0.0738 nm.

As shown in Fig. 3, defects are around the circumference of the nanotube for three situations: A, B, and C. Figures 5 and 6 show the critical bending buckling moments for zigzag (12,0) and armchair (7,7) nanotubes with different aspect ratios, respectively. The critical buckling moments and curvatures were obtained by the continuum model, in addition to our present model.

With increasing aspect ratio, shell and Euler modes will occur, respectively. When the Euler buckling mode occurs (aspect ratio of up to 30), the critical buckling moments and curvatures follow from the continuum model ($E = 1.07$ TPa, $t = 0.34$ nm). Therefore, we can calculate the critical buckling moments and curvatures by the continuum model simply enough for the long carbon nanotubes. Similar results can be seen

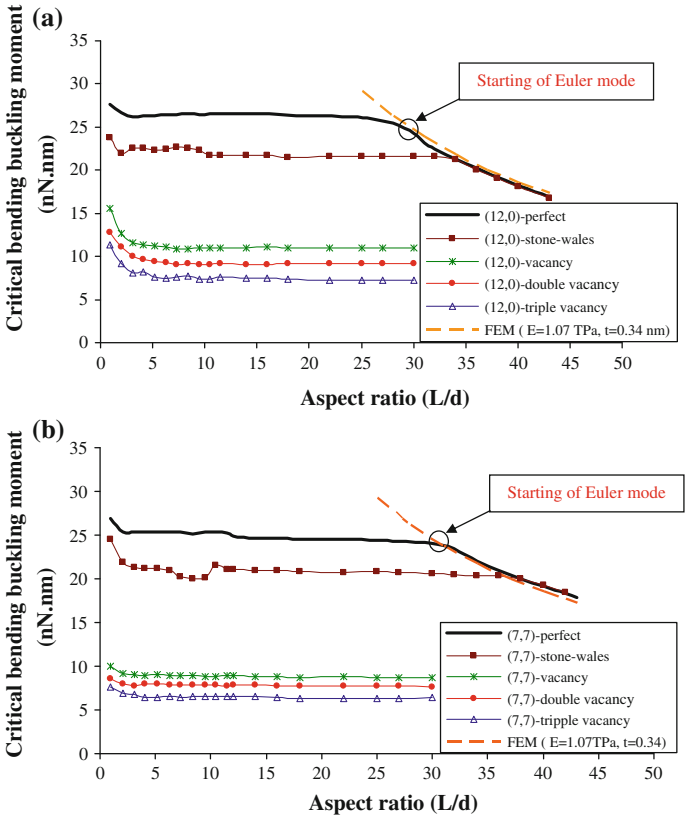

Fig. 5 Influence of the aspect ratio of (12,0) and (7,7) nanotube on the critical bending buckling moments

in other works such as the axial buckling behavior of carbon nanotubes in which by increasing the aspect ratio first they locally buckle and then globally buckle [15,16], and the torsional buckling behavior in which for slender SWCNTs with fixed diameter the critical torsional angle is approximately proportional to the length, consistent with the conventional shell theory [17]. It is also seen that the critical moments and curvatures are approximately constant when shell mode shapes occur. Then, with increasing nanotube aspect ratio and Euler mode shapes, critical moments decrease.

Types of vacancy and Stone–Wales defects for the study of defects in carbon nanotubes are illustrated in Figs. 7 and 8, respectively. Vacancies result from missing carbon atoms in the CNT walls. The defects included are single vacancies (one atom missing), tow opposite vacancies, double-vacancies (two adjacent atoms missing), and triple vacancies (three adjacent atoms missing). By removing the carbon atoms from the nanotube, all of the interactions (springs and connectors) between bonds will remove. Unlike the vacancy defects in which bonds have been removed, the carbon bonds in Stone–Wales defects will not remove but will rotate. All of the defects in Figs. 7 and 8 are situated at the middle of the nanotube. It is clear that the critical buckling moments and curvatures will decrease more for a triple vacancy than for the other tow vacancies, and vacancy defects have more effect than Stone–Wales defects in general.

The simulation results show that the influence of the location of the defect on the critical bending buckling moments and curvatures is significant. By displacing the defects at the circumference of the nanotube, we have found that the critical point for the existence of the defect is at the location C of the carbon nanotube. All of the defects in Figs. 5 and 6 are situated at the middle and location C of the nanotube.

As indicated in Figs. 5 and 6, the defects have a very weak effect on the critical buckling moments and curvatures when the Euler mode occurs. Of course, it should be noted that for defective nanotubes the Euler mode will happen later; it occurs at an aspect ratio of approximately 35 for a Stone–Wales defect. One can conclude from the above observations that it would be safer to choose long-length defective nanotubes.

The mode shapes according to the displacement contours are represented for various buckling modes of perfect zigzag nanotubes in Fig. 9. With increasing aspect ratio, the shell mode shapes are converted to the Euler mode shape. In addition, the mode shapes of defective nanotubes with a Stone–Wales defect (location B)

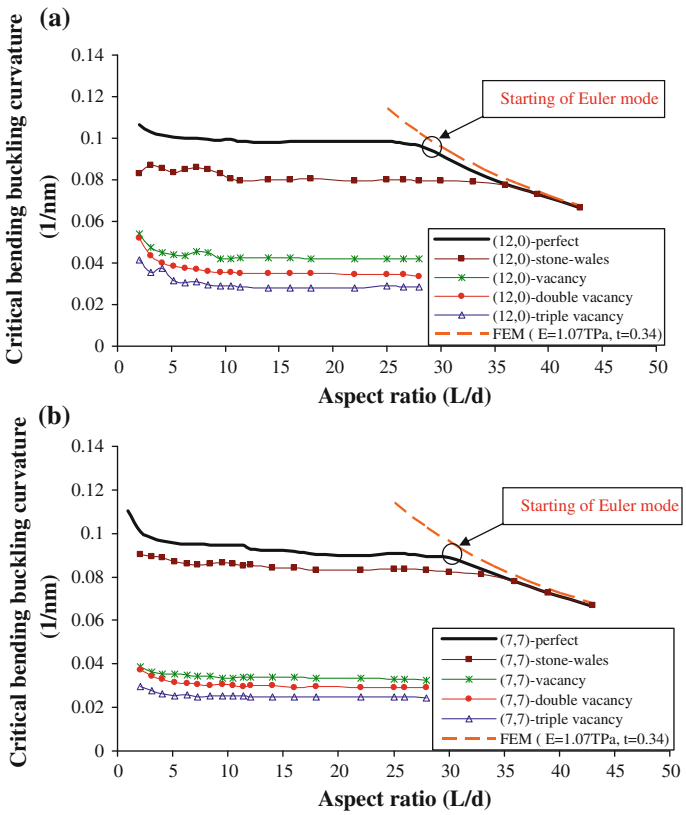

Fig. 6 Influence of the aspect ratio of a (12,0) and (7,7) nanotube on the critical bending buckling curvatures

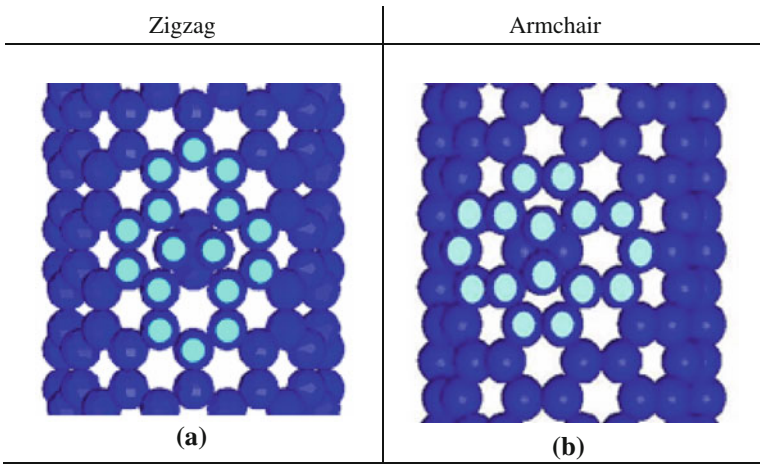

Fig. 7 Construction of a (12,0) zigzag (**a**) and a (7,7) armchair (**b**) SWNT with a Stone–Wales defect

for two different lengths of armchair nanotubes are compared. These defects will vary the mode shapes from 5.165 nm and larger. This length for zigzag nanotubes is larger than that for armchair nanotubes; this means that zigzag nanotubes are more resistant to defects than armchair nanotubes. The mode shapes of perfect zigzag and armchair nanotubes are similar; however, they are not similar when there are defects. The difference between the angles of defects in zigzag and armchair nanotubes may be one reason for this difference. Furthermore, the mode shapes of vacancy and Stone–Wales defects at the middle of the nanotubes are illustrated in Fig. 10. It can be deduced, with decreasing area of vacancy defect, that the distribution of load on the carbon atoms becomes more uniform.

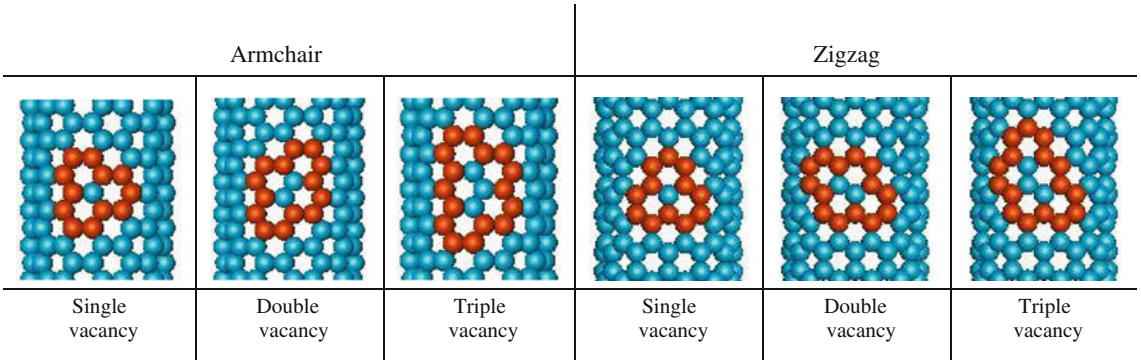

Fig. 8 Different vacancy defects used in the analysis

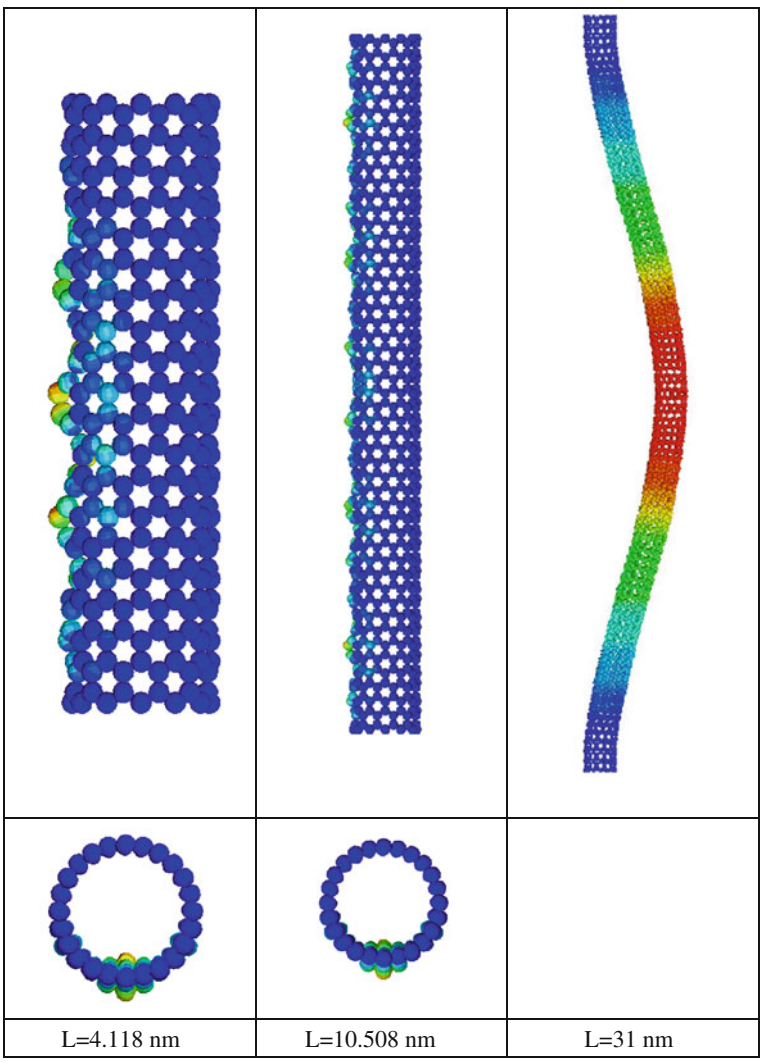

Fig. 9 The mode shapes of (12,0) SWCNTs under bending moment for various lengths

Figure 11 shows curves of the critical bending buckling moment versus the displacement of defects along the nanotube for different aspect ratios of nanotubes. The locations of the single vacancy defect are $L_0 = 0.9L$, $L_0 = 0.75L$, and $L_0 = 0.5L$, where L_0 is the distance of the defect from the load application point, and L is the length of the nanotube.

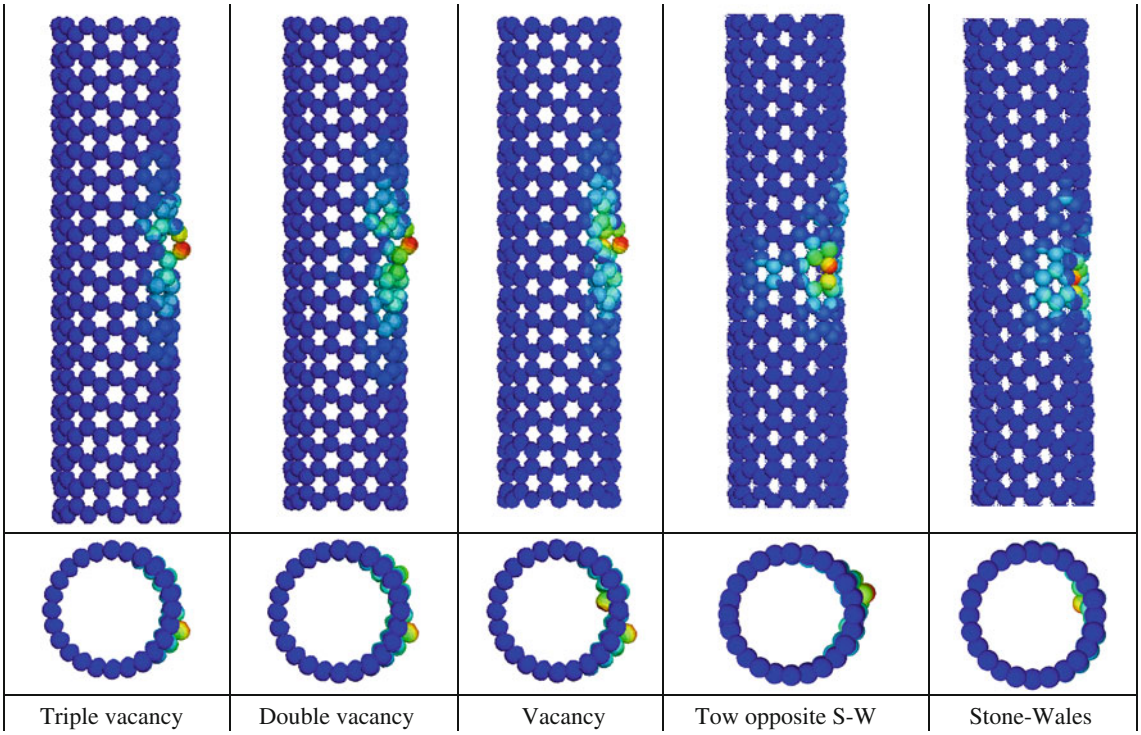

Fig. 10 Mode shapes according to displacement contours of defective nanotubes with various vacancies and Stone–Wales defects at the middle of the nanotube for zigzag ($L = 4.118$ nm) CNTs

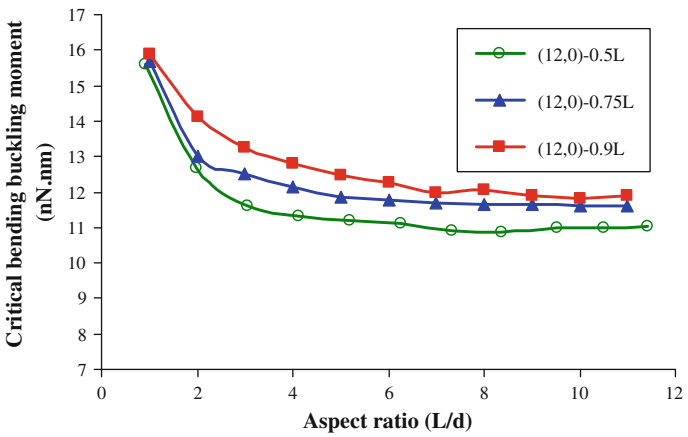

Fig. 11 Critical bending buckling moments for various locations of vacancy defects along zigzag CNTs

When the defect is located at mid-height, the cylindrical nanotube's buckling capacity is almost equivalent to the load level at which the first local buckling occurs. When the defect is located near the loaded end, a transition from the first local buckling mode to a higher local buckling mode would take place, which could significantly increase the nanotubes' buckling capacity.

Results indicate that with the displacement of the defect toward the load application point, the reduction in the critical buckling load will become minor; hence, the critical point for the existence of the defect is at the middle of the carbon nanotube.

The mode shapes of defective nanotubes with a single vacancy at different locations of the nanotubes are compared in Fig. 12. The displacement contour is uniformly distributed on the atoms at the regions around the defect when it is situated at the middle of the carbon nanotube.

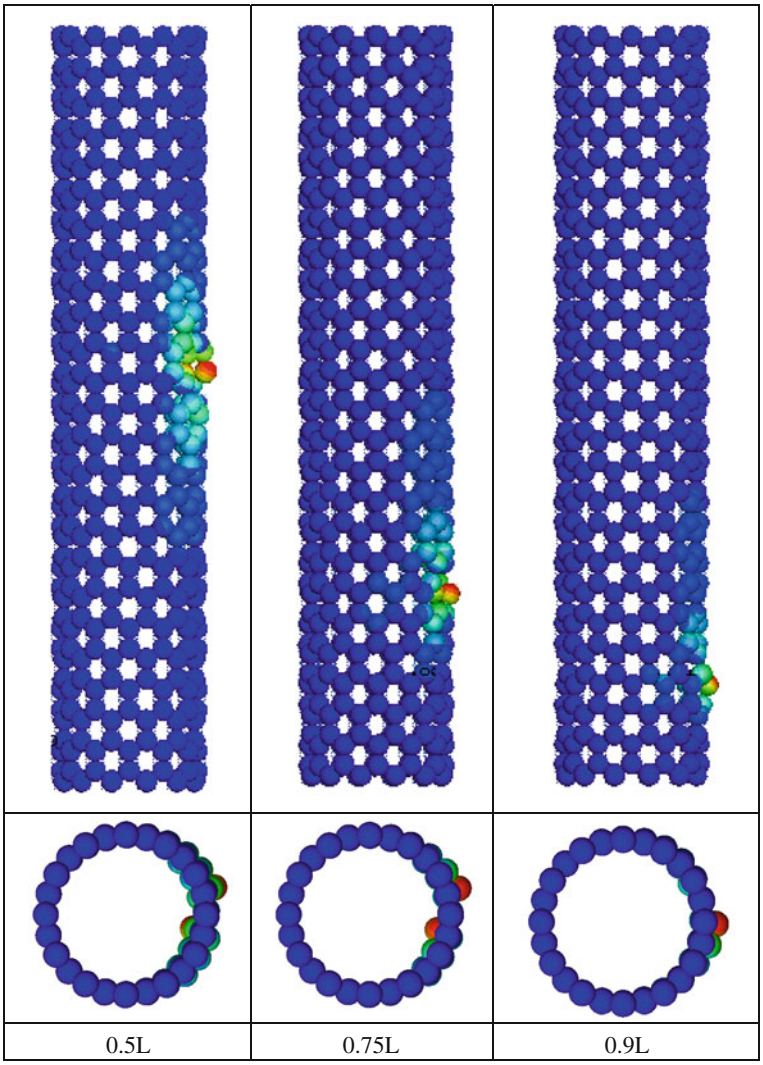

Fig. 12 Buckling mode shapes of zigzag CNT with a single vacancy at $L_0 = 0.9L$, $0.75L$ and $0.5L$

4 Conclusions

The effects of the type and location of vacancy and Stone–Wales defects on the bending buckling behavior of SWCNTs under bending moments were studied based on a structural mechanics approach using ABAQUS software. From these investigations, the following results can be drawn:

1. We can calculate the critical bending buckling moments and curvatures for sufficiently long nanotubes using simple continuum models.
2. The vacancy and Stone–Wales defects have a significant effect on the critical buckling moments when shell modes occur. This effect for a vacancy defect is more significant than for Stone–Wales defects.
3. The defects cause the Euler mode to occur later, and it would be safer to choose long-length defective nanotubes.
4. A double-vacancy decreases the critical buckling moment more than tow opposite vacancy defects.
5. The locations of defects on the nanotube have a significant effect on the critical buckling moments and curvatures of (12,0) and (7,7) CNTs such that the critical location of the defect is at the middle and location C of them.
6. The present structural model can be used for the prediction of the bending buckling behavior of SWCNTs due to the good agreement with the MD simulation.

References

1. Ijima, S.: Helical microtubules of graphitic carbon. Nature **354**, 56–58 (1991)
2. Wang, X., Wang, X.Y., Xiao, J.A.: A nonlinear analysis of the bending modulus of carbon nanotubes with rippling deformation. Compos. Struct. **69**, 315–321 (2005)
3. Yao, X., Han, Q., Xin, H.: Bending buckling behaviors of single- and multi-walled carbon nanotubes. Comput. Mater. Sci. **43**, 579–590 (2008)
4. Guo, X., Leung, A.Y.T., He, X.Q., Jiang, H., Huang, Y.: Bending buckling of single-walled carbon nanotubes by atomic-scale finite element. Compos. Part B Eng. **39**, 202–208 (2008)
5. Leung, A.Y.T., Guo, X., He, X.Q., Kitipornchai, S.A.: A continuum model for zigzag single-walled carbon nanotubes. Appl. Phys. Lett. **86**, 083110-1-3 (2005)
6. Odegard, G.M., Gates, T.S., Nicholson, L.M., Wise, K.E.: Equivalent-continuum modeling with application to carbon nanotubes. NASA/TM, 211454 (2002)
7. Han, Q., Lu, G., Dai, L.: Bending instability of an embedded double-walled carbon nanotube based on Winkler and van der Waals models. Compos. Sci. Technol. **65**, 1337–1346 (2005)
8. Sun, Y., Liew, K.M.: The buckling of single-walled carbon nanotubes upon bending: The higher order gradient continuum and mesh-free method. Comput. Methods Appl. Mech. Eng. **197**, 3001–3013 (2008)
9. Parvaneh, V., Shariati, M., Majd, A.M.: Investigation of defects effects on the buckling behavior of SWCNTs via a structural mechanics approach. Eur. J. Mech. A Solids **28**, 1072–1078 (2009)
10. Rappe, A.K., Casewit, C.J., Colwell, K.S. et al.: A full periodic-table force-field for molecular mechanics and molecular dynamics simulations. J. Am. Chem. Soc. **114**, 10024–10035 (1992)
11. Belytschko, T., Xiao, S.P., Schatz, G.C., Ruoff, R.S.: Atomistic simulations of nanotube fracture. Phys. Rev. B **65**, 235–430 (2002)
12. Cornell, W.D., Cieplak, P., Bayly, C.I. et al.: A second generation force-field for the simulation of proteins, nucleic-acids, and organic-molecules. J. Am. Chem. Soc. **117**, 5179–5197 (1995)
13. Yakobson, B.I., Brabec, C.J., Bernholc, J.: Nanomechanics of carbon tubes: instability beyond linear response. Phys. Rev. Lett. **76**, 2511–2514 (1996)
14. Cao, G.X., Chen, X.: Buckling of single-walled carbon nanotubes upon bending: molecular dynamics simulations and finite element methods. Phys. Rev. B. **73**(155435), 1–10 (2006)
15. Guo, X., Leung, A.Y.T., Jiang, H., He, X.Q., Huang, Y.: Critical strain of carbon nanotubes: an atomic-scale finite element study. J. Appl. Mech. Trans. ASME **74**, 347–351 (2007)
16. Leung, A.Y.T., Guo, X., He, X.Q., Jiang, H., Huang, Y.: Postbuckling of carbon nanotubes by atomic-scale finite element. J. Appl. Phys. **99**, 124308 (2006)
17. Leung, A.Y.T., Guo, X., He, X.Q.: Torsional buckling of single-walled carbon nanotubes. Comput. Methods Appl. Sci. **9**, 1–8 (2008)